JAES | JOURNAL OF APPLIED ENGINEERING SCIENCE | www.engineeringscience.rs
ISTRAŽIVANJA I PROJEKTOVANJA ZA PRIVREDU

Indexed by

CONTRIBUTION TO THE INVESTIGATION OF THE INFLUENCE OF TIRE NON-UNIFORMITY ON THE LATERAL TIRE CHARACTERISTICS

Milena Žunjić
University of Belgrade, Faculty of Mechanical Engineering

Miroslav Demić
Academy of Engineering Sciences of Serbia, Belgrade

Branislav Rakićević
University of Belgrade, Faculty of Mechanical Engineering

Branislav Đorđević
University of Belgrade, Faculty of Mechanical Engineering

Key words: *tires, models, lateral characteristics, 3D Fourier transformation*
doi:10.5937/jaes0-32961

Cite article:

Žunjić M., Demić M., Rakićević B., Đorđevićr B. (2022) CONTRIBUTION TO THE INVESTIGATION OF THE INFLUENCE OF TIRE NON-UNIFORMITY ON THE LATERAL TIRE CHARACTERISTICS, *Journal of Applied Engineering Science*, 20(2), 562 - 570, DOI:10.5937/ jaes0-32961

Online aceess *of full paper is available at: www.engineeringscience.rs/browse-issues*

Istraživanja i projektovanja za privredu
Journal of Applied Engineering Science

Original Scientific Paper

doi:10.5937/jaes0-32961

Paper number: 20(2022)2, 962, 562-570

CONTRIBUTION TO THE INVESTIGATION OF THE INFLUENCE OF TIRE NON-UNIFORMITY ON THE LATERAL TIRE CHARACTERISTICS

Milena Žunjić[1,]*, Miroslav Demić[2], Branislav Rakićević[1], Branislav Đorđević[1]
[1]University of Belgrade, Faculty of Mechanical Engineering
[2]Academy of Engineering Sciences of Serbia, Belgrade

Tire models are widely used in research in the field of vehicle dynamics and noise, and especially in the simulation of their movement under the action of forces and moments. In general case, we distinguish theoretical models defined on the basis of tire construction and empirical or semi-empirical models based on experimental tests. In addition, a combination of these two types of models can also produce tire models. In practice, there is a very wide range of mathematical tire models defined using finite element analysis, by approximation of polynomials of different degrees, by approximation of magic formula, etc. In this paper, an attempt is made to calculate non-stationary lateral characteristics of tires on the basis of experimental stationary lateral characteristics, using two-parameter higher level polynomials. This polynomials define the tire lateral characteristics, and take into account their non-uniformity. More specifically, the lateral characteristics are approximated as a function of the dynamic change of the slip angle, radial load due to tire non-uniformity and time.

Key words: tires, models, lateral characteristics, 3D Fourier transformation

INTRODUCTION

Tire models are widely used in research in the field of vehicle dynamics and noise, and especially in the simulation of their movement under the action of forces and moments. Forces and torques are functions of different slip parameters, such as tire slip angle. In general case, tire models can be divided in two groups: theoretical (based on tire construction) and empirical / semi-empirical (based on experimental tests). In addition, a combination of these two types of models can also produce tire models [1-11]. In practice, there is a very wide range of mathematical tire models defined using finite element method, by approximation of polynomials of different degrees, by approximation of magic formula, etc. [1-11]. It is noted that use of the magic formula is widespread today, but it should be known that it includes numbers of slip parameters that define lateral force or self aligning torque [1-3]. Confirm of all slip parameters precludes the successful application of the magic formula for modeling the lateral and tangential characteristics of tires. Reference [9] explains that vertical displacements of the center of the wheel lead to a change in lateral characteristics (in this case, lateral forces), Figure 4. In practice, this change of vertical impulse may occur due to a change of radial stiffness along the circumference of the wheel, and as a consequence of tire non-uniformity. During the rolling of a non-uniform tire, the parameters used to assess the non-uniformity of the tire are change (changes in radial and lateral force, conical and angular effect) [5]. Therefore, it was of interest to investigate how the variable radial force from non-uniformity affects on the lateral characteristics of the tires. It was considered expedient to develop a method for the analysis of the

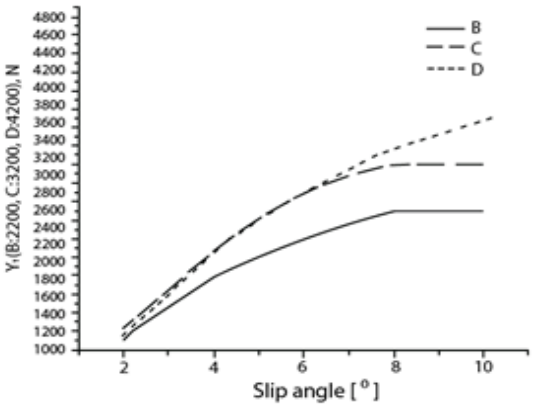

Figure 1: Lateral forces as a function of side slip angle and tire radial force (Radial foce during testing, B-2200, N; C-3200, N and D-4200, N), [6]

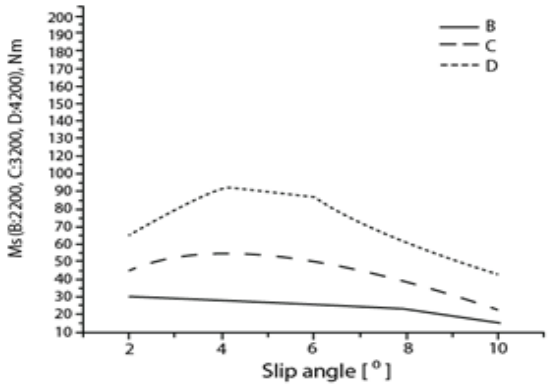

Figure 2: Self aligning torques as a function of side slip angle and radial force (Radial force during testing, B-2200, N; C-3200, N and D-4200, N), [6]

*mzunjic@mas.bg.ac.rs

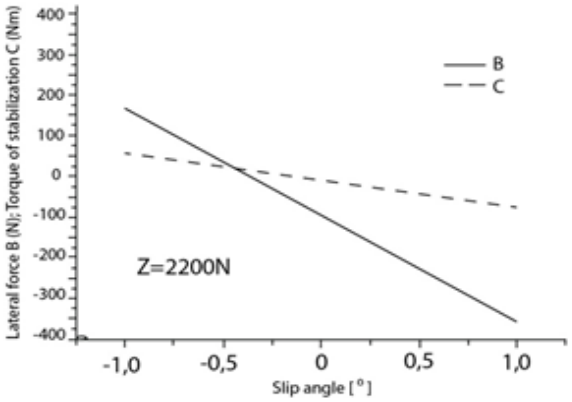

Figure 3: Lateral force and self aligning torque as a function of side slip angle, [6]

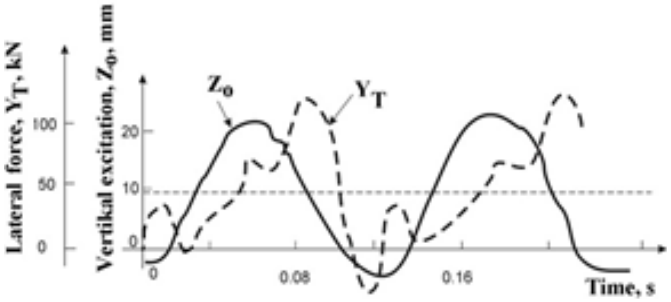

Figure 4: Lateral force as a function of radial oscillatory excitation of a wheel, [9]

influence of tire non-uniformity on their lateral characteristics. In this paper, a method was developed that can have a general application, but due to the lack of data for larger tires, is illustrated by the example of a smaller tire that was used in Zastava 101 vehicles (now in smaller city vehicles). Specifically, were used the test results of tires manufactured in Trayal company, 145R13 74S on rim 41/2 JX 12 realized at the Technical University of Munich [4, 6]. 14 tires were tested, which is acceptable for statistical reliability. The obtained results are shown by continuous curves, however, in [6] due to the identification of parameters, their digitization was performed, so that they are shown by broken curves. That tire is intended to be operated at a radial load of up to 3200 N and air pressure of 1,8 bar. The tests were performed at constant radial loads of 2200, 3200 and 4200 N, with a variation in slip angle from 0 to 10°, with increments of 2°. The results of the experimental laboratory tests on the MTS test roller are showed in those figures. By analyzing the data in Figures 1 and 2, it can be established that lateral forces and self aligning torque are nonlinearly dependent on slip angle and radial load, and the limit values defined by the adhesion conditions are not explicitly showed in Figures 1 and 2. In addition to data shown in Figures 1 and 2, the tests were also performed while varying the slip angle in the range from -1° to +1°, with the results shown in Figure 3, for radial load of 2200 N. It can be seen from the figure that the lateral force and the self aligning torque in this test have values different from zero, when slip angle is equal to zero. This fact must be taken into account in tire design process. The radial oscillatory excitations influence the lateral force change [9], Figure 4. Analyzes [4,6] have shown that data presented in Figures 1 and 2 can be approximated with acceptable accuracy by the expressions:

$$Y_T = (x_{1y} + x_{2y}\delta + x_{3Y}\delta^2 + x_{4Y}\delta^3)* \\ *(x_{5Y} + x_{6Y}Z_T), \\ M_s = (x_{1M} + x_{2M}\alpha x_{3M}\delta^2 + x_{4M}\delta^3)* \\ *(x_{5M} + x_{6M}Z_T) \quad (1)$$

Where:

Y_T [N] - lateral force,

M_s[Nm] - tire self aligning torque,

x_{ry} and x_{rM} (r=1÷6) - parameters given in Table 1,

δ[rad] - side slip angle,

Z_T[N] - radial tire load.

The unknown parameters in expression (1) were calculated using optimization methods aimed at minimizing the difference of the squares between the experimental data from the test table and the data obtained on the basis of expression (1). As these procedures are known from [12]. The coefficients appearing in expression (1) for the tire tested are shown in Table 1 [6].

Table 1: Model parameters (1)

r	Parameters x_{ry} for Y_T	Parameters x_{rM} for M_s
1	- 0.6990927292314295	-0.2309627295128
2	17.88073727024941	1.4071072704822
3	-1.176192729518429	-0.2300527295150
4	0.0202172704850190	0.0101072704849
5	23.07542727007415	-20.013622729274
6	0.0044575193552971	0.0141311984024

Expression (1) is also digitalized with the help of a PC calculated value of lateral force and self aligning torque, for the area of definition of variables (slip angles, radial force). The obtained results are presented in the form of 3D diagrams in Figure 5 and 6.

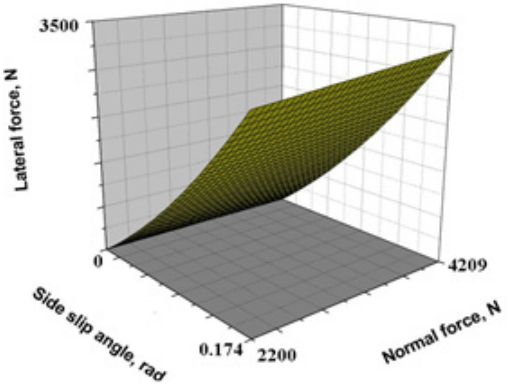

Figure 5: Lateral force as a function of side slip angle and radial force

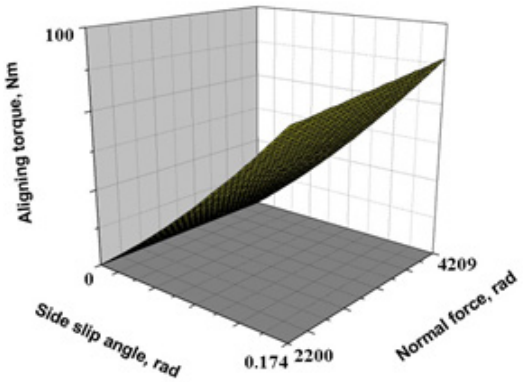

Figure 6: Aligning torque as a function of side slip angle and radial force

As mentioned earlier, the lateral force and stabilization momentof the tirs from Figures 1 and 2 were modeled with acceptable accuracy, with expression 1. Analyzes [4, 6] showed that the approximation error in the boundary areas of radial force and steering angle is less than 4%. In [4, 6] the results of the approximation are shown by 2D diagrams, while in this paper the same results are shown in Figures 5 and 6 by 3D diagrams. Figures 5 and 6 show that the lateral characteristics of the tires depend on the steering angle and radial force. The analysis of expression (1) shows that the radial force, the slip angle and the coefficients calculated using the optimization method figure in expression (1). During the testing of tires whose lateral characteristics are shown in this paper, the radial force was constant, and the steering angle was gradually changed. In this paper, an attempt is made to investigate how the dynamic radial force affect the lateral characteristics of tires, so it was considered expedient to include in expression (1) the variation of radial force from tire non-uniformity. The reason for applying the radial force variation is the consequence that it is not possible to produce an ideal tire, so, in practice, structural errors are present, which are manifested by changes in shape, uneven tire stiffness along the circumference, the appearance of a conical and angular effect, etc. [5,11]. This is manifested by variations of forces and torque when tire is rolling. When measuring the lateral characteristics of tires, tires with allowed values of non-uniformity are most often used, so this influence on the lateral characteristics is not taken into account. In order to provide an easier understanding of the text below, a brief account of the tire nonuniformity theory is given. For illustration, a schematic display of a variation of radial nonuniformity of tire was given in Figure 7 [5]. In figure, the following terms are used: reference angle - Θ, current value of force – TS, force average value - SVS, force variation - VS, peak-to-peak value of force - 2Ai. As these terms are explained in detail in [5], there will be no more words here, but only the basic relationships will be given. The dependency between the variation of the peak-to-peak first harmonic force variation and peak-to-peak radial force variation is presented in Figure 8. The force variation is defined with the following expression:

$$VS(\theta) = TS(\theta) - SVS \tag{2}$$

The force variation can be expressed in function of the reference angle by developing into a Fourier series [5]:

$$VS(\theta) = \sum_{i=1}^{n} \left[A_i \cos(\theta_i - \varphi_i \right] \tag{3}$$

Where:

A_i - amplitude of harmonics,

φ_i - harmonic phase,

i - number of radial force harmonics,

n - number of harmonics of the radial force.

Research has shown that the first three harmonics are the most pronounced and can be statistically expressed as functions of the first harmonic. Bearing in mind the findings from [13-15], these functions for 145 SR13 tire are:

A1=45 N, A2=0.9 A1, A3=0.72 A1.

The following phases of harmonics are assumed for dynamic simulations: φ1=0 rad, φ1=π rad

$$\varphi_3 = \frac{2\pi}{3} \text{ rad}$$

With that in mind, radial force in function of time can be defined with the following expression (4):

$$Z_T = G_{st} + FV(\theta) \tag{4}$$

Where: G_{st} is wheel static load (in this case G_{st}=2200 N) and Θ is reference angle defined by:

$$\theta_i = \frac{i \cdot v \cdot t}{3.6\, r_d} \tag{5}$$

Where:

i - number of harmonics,

v - vehicle speed on roller test bench (in this case 80 km/h),

r_d - dynamic tire radius (in this case 0.270 m).

Figure 3 indicates that changes in the side slip angle causes the lateral characteristics to change, we will assume the side slip angle in the form:

$$\delta = \delta_{\max} \sin\left(\frac{2\pi \cdot t \cdot \delta_v}{i_u}\right) \tag{6}$$

Where:

δ_{max}[rad] - maximum side slip angle of tire (in this case 0.02 rad),

t[s] - time,

δ_v [rad] - steering wheel angle,

i_u- transmission ratio of steering system (in this case 2).

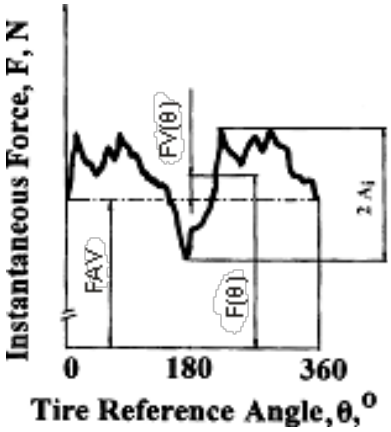

Figure 7: Basic definitions of radial nonstationarity of tire [5]

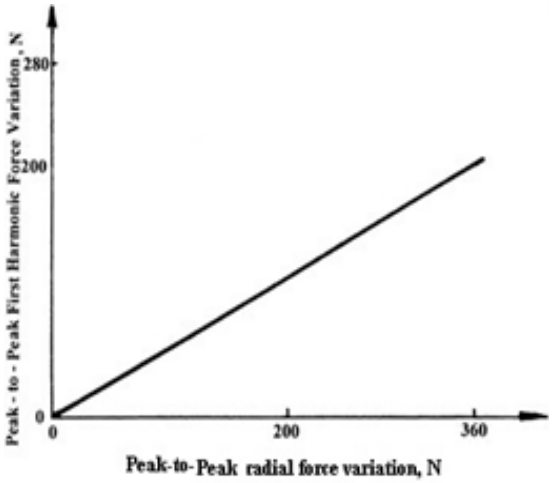

Figure 8: Statistical dependence of the variation of first harmonic variation and radial force variation [5]

Oscillatory motions of motor vehicles are often considered in the frequency domain [13 - 19] it was decided to calculate the Fourier transform spectra of the lateral characteristics of the tires. They depend on three variables in this case, so it is necessary to use 3D Fourier transform. Therefore, we will briefly look at the definition of multidimensional Fourier transform. Based on [20-23], the general case of multidimensional Fourier transform is given by:

$$Ff\left(\xi_1,\xi_2...\xi_n\right)= \\ =\int_{R^n} e^{-2\pi i\left(x_1\xi_1+x_2\xi_2+....+x_n\xi_n\right)} f\left(x_1,x_2...x_n\right)dx_1dx_2...dx_n \quad (7)$$

Where:

$f(x_1,x_2,\ldots,x_n)$ - a function of n variables whose Fourier transform is calculated,

$x_1,x_2,\ldots,x_n$ - variables,

$\xi_1, \xi_2,\ldots,\xi_n$ - circular frequencies,

$\int_R$ multiple integral corresponding to the number of variables (e.g. for 2D - double integral, for 3D triple integral, etc.),

R^n- the domain (in theory -∞, +∞, in practice the limit values). Obviously, based on the general expression (7), the expression for 3D Fourier transform can be written [20]. It is noted that expression (7) can also be written in a discrete form, which will not be done here. It should be emphasized that multidimensional Fourier transform is a very complex function, and is usually used in the literature: 2D for photo processing, and 3D for plate vibration processing [21-22]. It is emphasized that visualization is difficult for n<2, which significantly reduces the possibility of its application [22]. Analyzes [21,22] have shown that the phase angles of the mentioned transformations do not provide usable information about the character of the process, so it is recommended, that the spectrum of the observed magnitudes are used exclusively for these purposes. Therefore, the analysis of the spectrum modules (of 3D Fourier transforms), was calculated using the program that was realized in Pascal for the purpose of this paper.

METHOD AND DATA ANALYSIS

The upgraded model (1) includes three variables (time, dynamic radial force and side slip angle). It should be emphasized that the spectral data of the displayed files in digital form can be used for further research without visualization. The lateral characteristic of the tires are shown in this way. The following data were used during the dynamic simulation: h_t=0,02 s, h_δ=0,02 rad, h_z=5, N in N_t=64, N_δ=64 and N_t=32 points. This enabled the reliability of the results of the dynamic simulation in the field [19]:

- time 0,781 - 25 Hz,
- side slip angle 0,781 - 25 rad^{-1},
- normal reaction 0,00625 - 0.1 N^{-1},

which is acceptable for the lower frequency range.

Analysis of digital data on 3D Fourier transform modules revealed that there are non-zero values throughout the volume of the square within the scope of the variables mentioned, which implies that 4D graphics, which is very complex, should be used for visualization. Therefore, the change of lateral characteristics is shown for three boundary planes of the square, both for the initial and final values of the analyzed sizes, thus creating the possibility of using 3D graphics, which is far simpler than 4D graphics. Border plane projections are defined:

XY plane: $f\left(i=1,\ N_t;\ j=1,\ N_\delta;\ k=1,\right)$

YZ plane: $f\left(i=1,\ N_t;\ j=1;\ k=1,\ N_z\right)$

XZ plane: $f\left(i=1;\ j=1,\ N_\delta;\ k=1,\ N_z\right)$

Where, N_t, N_δ and N_z represent the number of points in the direction of the corresponding axes (time, side slip angle, normal reaction) in which the lateral characteristics are defined. When it comes to spectra, due to the

FFT algorithm used, the upper limit should be divided by 2 [23]. Based on expressions (1-6) it is found that the lateral forces and the self aligning torque have a similar shape. Therefore, it was not necessary to show 3D diagrams for the complete lateral characteristics, already shown in Figure 9 to 15 for boundary surfaces. Figures 9 to 15 show the dependences of lateral characteristics change on time, side slip angle and radial load. For more detailed analysis, a 3D Fourier transform was performed, and the spectral modules for the boundary surfaces are shown in Figure 16 to 22. From the mentioned Figures, it is clearly observed that the spectra depend on all three variables. For further analysis, the hypothesis was adopted: If the originals and spectra of the lateral characteristics for the boundary conditions differ from each other, then they change over the entire volume of the cuboid. To confirm the hypothesis adopted, the RMS of the lateral characteristics for cut-off values of the data used are presented in Table 2.

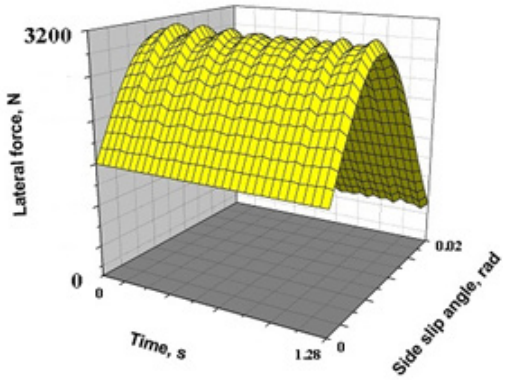

Figure 9: Lateral force as a function of time and side slip angle[expression(8)]

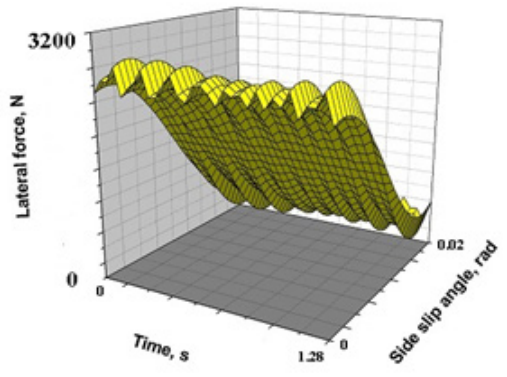

Figure 10: Lateral force as a function of time and side slip angle [expression (9)]

Figures 9 and 10 show the lateral forces depending on the time and angle of conduct, for the boundary conditions defined by expressions (8) and (9). By analyzing Figures 9 and 10, and having in mind the adopted hypothesis as well as expressions (8) and (9), it is obvious that the lateral force changes according to the volume of the frame. The same is true for Figures 11 and 12, the limit values given by expressions (10) and (11), which show the dependence of the lateral force on time and radial force.

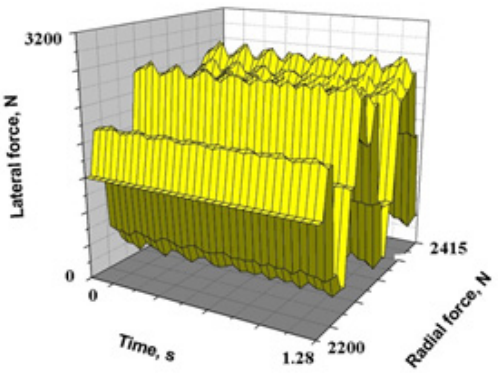

Figure 11: Lateral force as a function of time and radial force [expression (10)]

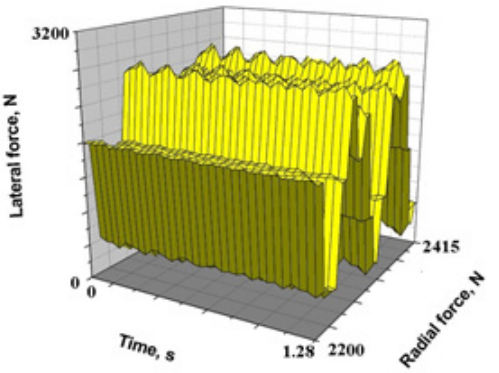

Figure 12: Lateral force as a function of time and radial force [expression (11)]

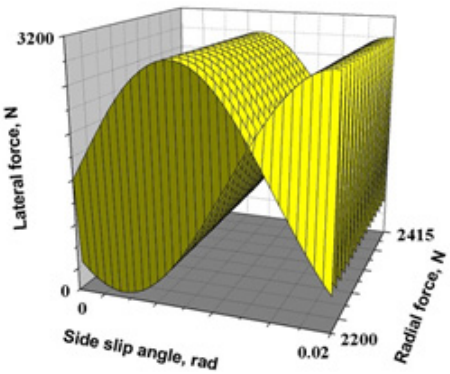

Figure 13: Lateral force as a function of the side slip angle and radial forces [expression (12)]

Figures 13 and 14 show the lateral forces depending on the side slip angle and the radial force, for the boundary conditions defined by expressions (12) and (13). It is obvious that in this case, too, there is a change in the volume of the square. The same applies to Figures 15 and 16, which show the lateral force depending on the side slip angle and the radial force [boundary conditions defined by expressions (14) and (15)]. Analyzes have

shown that the influence of the side slip angle and radial force also exists at the moment of stabilization. Figure 15 shows the moment of stabilization depending on the time and side slip angle, for the case of boundary conditions defined by expression (14).

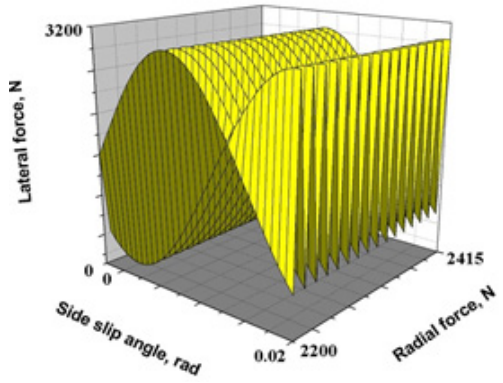

Figure 14: Lateral force as a function of the side slip angle and radial force [expression (13)]

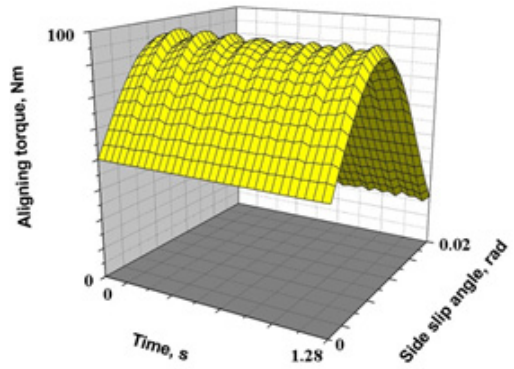

Figure 15: Self aligning torque as a function of time and side slip angle [expression (14)]

Figures 16 and 17 show the lateral force depending on the frequency in the time domain and the side slip angle, for the boundary conditions defined by expressions (15) and (16). By analyzing Figures 16 and 17, and in relation to outputs (15) and (16), it is obvious that the modulus of the lateral force changes according to the frame volume. The same is true for Figures 18 and 19, [limit values given by expressions (17 and 18)], which show the change of lateral force with the change in frequency in the time domain of the radial force. Figures 18 and 19 show the changes in lateral force depending on the frequency in the time domain and the radial force domain, for the boundary conditions defined by expressions (17) and (18). By analyzing Figures 18 and 19, and having in mind the adopted hypothesis as well as expressions (17) and (18), it is obvious that the lateral forces change according to the volume of the frame. The same comment applies to Figures 20 and 21, [limit values given by expressions (19 and 20)], which show the change in lateral force with the change in frequency in the domain of radial force and the domain of the side slip angle.

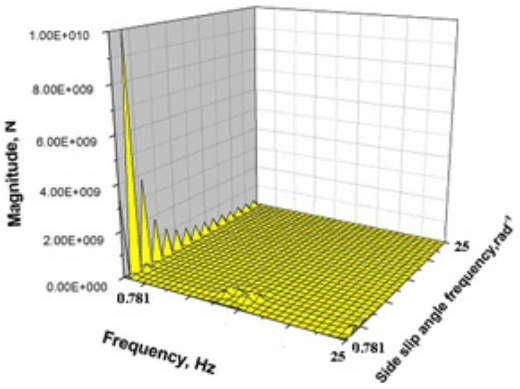

Figure 16: Mode of the lateral force spectrum as a function of time and side slip angle [expression (15)]

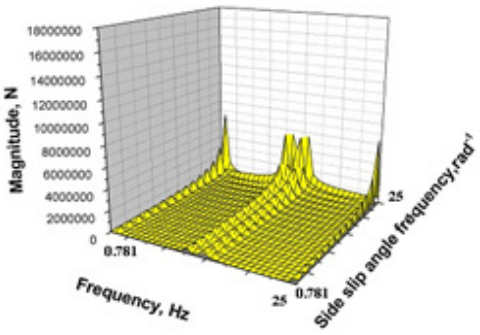

Figure 17: Mode of the lateral force spectrum as a function of the time and side slip angle [expression (16)]

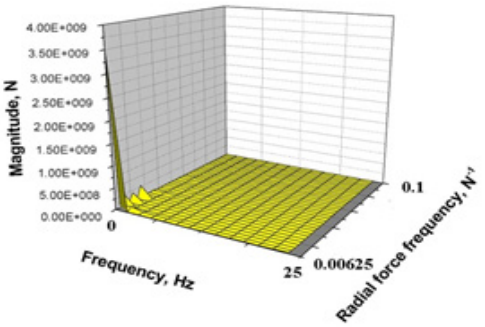

Figure 18: Lateral force spectrum mode as a function of time and radial force [expression (17)]

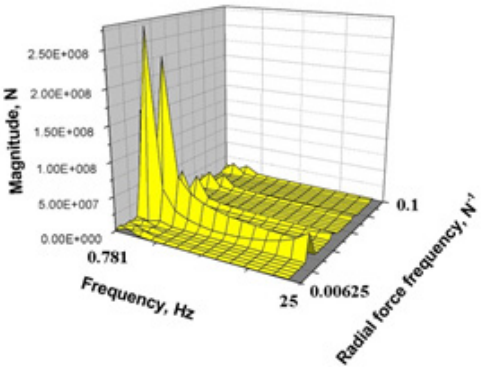

Figure 19: Lateral force spectrum mode as a function of time and radial force [expression (18)]

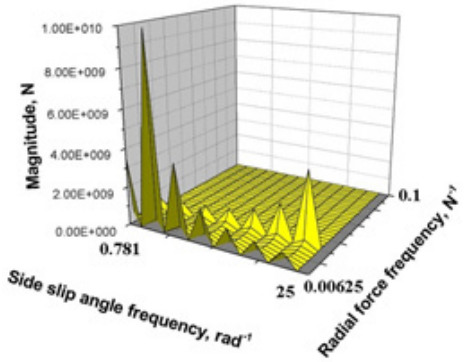

Figure 20: Mode of the lateral force spectrum as a function of the side slip angle and radial force [expression (19)]

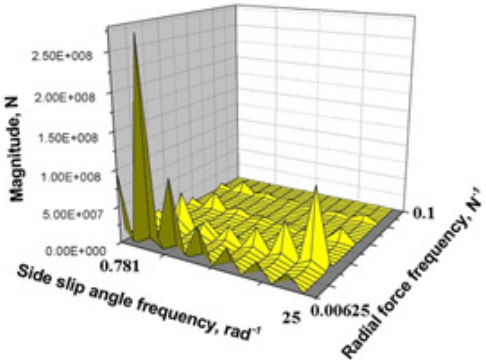

Figure 21: Mode of the lateral force spectrum as a function of the side slip angle and radial force [expression (20)]

Figure 22 shows the change in the moment of stabilization as a function of participation in time and side slip angle (boundary conditions given by expression 21). Analysis of the data from the mentioned figure shows that the moment changes, and detailed analyzes of all spectra (partially shown in Figure 22) showed that the moment changes over the entire volume of the square, as was the case with the lateral force. To confirm the adopted hypothesis, the RMS side characteristics for the limit values of the data used were calculated and shown in Table 2.

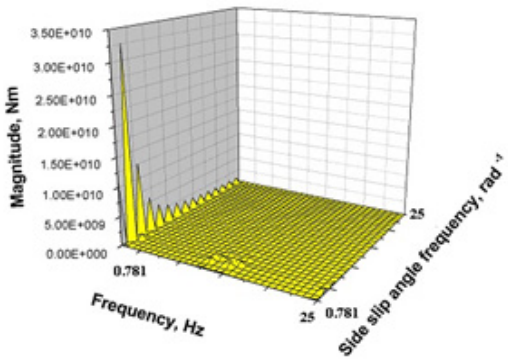

Figure 22: Mode of the spectrum of the moment of stabilization as a function of time and side slip angle [expression (21)]

Table 2: RMS spectra of 3D transformation modules

XY plane Y_t/M_s	XZ plane Y_t/M_s	YZ plane Y_t/M_s
(k=1) 363441417.76393/ 1179911137.90093	(j=1) 157528745.08428/ 490219744.32440	(j=1) 710302409.58263/ 2310446844.17760
($k=N_z$) 1504951.08034/ 4908237.95422	($j=N_\delta$) 22360809.44493/ 72941432.42647	($i=N_t$) 20061245.22244/ 65281010.79613

$$f\left(i=1,\ N_t;\ j=1,\ N_\delta;\ k=1\right) \tag{8}$$

$$f\left(i=1,\ N_t;\ j=1,\ N_\delta;\ k=N_z\right) \tag{9}$$

$$f\left(i=1,\ N_t;\ j=1;\ k=1,\ N_z\right) \tag{10}$$

$$f\left(i=1,\ N_t;\ j=N_\delta;\ k=1,\ N_z\right) \tag{11}$$

$$f\left(i=1;\ j=1,\ N_\delta;\ k=1,\ N_z\right) \tag{12}$$

$$f\left(i=N_t;\ j=1,\ N_\delta;\ k=1,\ N_z\right) \tag{13}$$

$$f\left(i=1,\ N_t;j=1,\ N_\delta;\ k=1\right) \tag{14}$$

$$f\left(i=1,\ \frac{N_t}{2};j=1,\ \frac{N_\delta}{2};\ k=1\right) \tag{15}$$

$$f\left(i=1,\ \frac{N_t}{2};j=1,\ N_\delta,\ k=\frac{N_z}{2}\right) \tag{16}$$

$$f\left(i=1,\ \frac{N_t}{2};j=1,\ k=1,\frac{N_z}{2}\right) \tag{17}$$

$$f\left(i=1,\ \frac{N_t}{2};j=\frac{N_\delta}{2},\ k=1,N_z\right) \tag{18}$$

$$f\left(i=1;j=1,\ \frac{N_\delta}{2};\ k=1,\frac{N_z}{2}\right) \tag{19}$$

$$f\left(i=1,\ \frac{N_t}{2};j=1,\ \frac{N_\delta}{2};\ k=1\right) \tag{20}$$

Based on data in Table 2, it is concluded that the side-effect spectra modules differ for the boundary surfaces of the cuboid. This confirms the accepted hypothesis that they change throughout the volume, which may justify the application of 3D transformation. Earlier, we pointed out that 3D Fourier transform requires large memory for storage. Therefore, higher order 3D and Fourier transforms have not found wider practical application in practice. We can confirm that expressions (1 to 6) Finally, we can argue that (expressions 1-6) allow the introduction of variable radial force due to non-uniformity in the analysis of lateral characteristics of tires. In the following period, experimental research should be performed in order to verify the method used. The introduction of variable radial force due to tire non-uniformity in expression (1), as well as a detailed analysis of the results of dynamic simulation showed that the influence of time, angle and radial force on lateral force, stabilization moment and exists over the entire volume of the square (parameter definition area). The influence is investigated in this paper at lower frequencies in time, and in the frequency domains of radial force and side slip angle. For research in higher frequency domains, it is necessary to perform additional experimental research.

CONCLUSION

The introduction of variable radial force due to non-uniformity of tires in expression (1), as well as a detailed analysis of the results of dynamic simulation showed that the influence of time, side slip angle and radial force on lateral force, stabilization moment exists over the entire volume of the square. The influence was checked in this paper at lower frequencies in time, as well as in the frequency domains of radial force and angle of conduct. For research in higher frequency domains, it is necessary to perform additional experimental research. This impact is analyzed at lower frequencies, while additional studies are required to analyze the impact at higher frequencies.

ACKNOWLEDGEMENT

The research presented in this paper is funded by the Ministry of Education, Science and Technological Development of the Republic of Serbia under agreement No. 451-03-9/2021-14/200105 dated 5.2.2021.

REFERENCES

1. Oritz, A. at all. (2006). An easy procedure to determine Magic Formula parameters: a comparative study between the starting value optimization technique and the IMMa optimization algorithm, Vehicle System Dynamics, Vol. 44, No 9, pp. 689-718.
2. Pacejka, H. B., Bekker, E. (1993). The Magic Formula Tire Model, Vehicle System Dynamics, 21, pp. 1-18.
3. Pacejka, H. B.: and Besselink, I. J. M. (1997). Magic Formula tyre model with transient propoertis, Vehicle System Dynamics Supplement, 27, pp. 234-249.
4. Demić M. (1985). Contribution to modelling of stationary lateral tire characteristics, ISATA, Graz.
5. Demić, M. (1999). The Definition of the Tires Limit of Admissible Nonuniformity by Using he Vehicle Vibratory Model, Vehicle System Dynamics, 31.
6. Demić M. (2013). Prilog identifikaciji modela stacionarnih bočnih karakteristika pneumatika, Tehnika-Mašinstvo, Vol. 62, Br 4, str. 653-658.
7. Genta A. (2003) Motor Vehicle Dynamics, Politecnika di Torino.
8. Gillespie T. D. (1992) Fundamentals of Vehicle Dynamics, SAE.
9. Ellis, J. R. (1973) Vehicle Dynamics, Business Books, London.
10. Miliken W., Miliken D. (1995) Race Car Dynamics, SAE.
11. Mitschke M. (1972). Dynamik der Kraftfahrzeuge (in German), Springer Verlag.
12. Bunday P.(1984) Basic optimisation methods. Spottiswoode Ballantyne, Colchester London.
13. 13. Meng Du. (2020). A Study on the Influence of Tire Speed and Pressure on Measurement Parameters Obtained from High-Speed Tire Uniformity Testing Licensee MDPI, (http://creativecommons.org/licenses/by/4.0/).
14. Doria1, A. at all. (2016). Identification of the Mechanical Properties of Tires for Wheelchair Simulation, The Open Mechanical Engineering Journal, 2016, 10, 183-200, available at: www.benthamopen.com/TOMEJ/, DOI: 10.2174/1874155X01610010183
15. Sina, N. at all. (2014). Excitation Behavior of Tire and Wheel Assembly Faults in Shape of Non-uniformity in a Vehicle, 8th Condition Monitoring & Fault Diagnosis Conference February, Sharif University of Technology, Iran.
16. Peng, C. at all.(1994). Lateral tyre dynamic characteristics, Journal of Terramechanics Volume 31, Issue 6, Pages 395-414.
17. Parczewski, K., Wnęk, H. (2015). The tyre characteristics of the physical model used to investigate the lateral stability of a vehicle, https://journals.sagepub.com/doi/abs/10.1177/0954407014563734?journalCode=pidb
18. Hassan, M. at all. (2020). Advanced study of tire characteristics and their influence on vehicle lateral stability and untripped rollover threshold, Alexandria Engineering Journal 59, 1613–1628.

19. Doumiati, M. at all. (2010). A method to estimate the lateral tire force and the sideslip angle of a vehicle: Experimental validation, American Control Conference Marriott Waterfront, Baltimore, MD, USA, June 30-July 02.
20. EE261 - The Fourier Transform and its Applications, https://see.stanford.edu/
21. Gonsales, C.R., Woods, E.R.(1980). Digital Image processing, Prentice Hall, New Jersey.
22. Kuroki, N. ”FFT2D” software (2017) http://cas.eedept.kobeu.ac.jp/WelcomeES1/OpenSoft/FFT2D/index_en.html.
23. Bendat J.S., Piersol A.G. (2000), Random Data-Analysis and measurement procedures. London: John Wiley and Sons.

Paper submitted: 02.11.2021.
Paper accepted: 10.12.2021.